Theoretical Analysis and Optimization of a Gloved Hand–Arm System

Oreoluwa Alabi
Department of Mechanical Engineering,
Virginia Polytechnic Institute and
State University,
Blacksburg, VA 24061

Sunit K. Gupta
Department of Mechanical Engineering,
Virginia Polytechnic Institute and
State University,
Blacksburg, VA 24061

Oumar Barry[1]
Department of Mechanical Engineering,
Virginia Polytechnic Institute and
State University,
Blacksburg, VA 24061
e-mail: obarry@vt.edu

Studies have shown that isolators in the form of antivibration (AV) gloves effectively reduce the transmission of unwanted vibration from vibrating equipment to the human hand. However, as most of these studies are based on experimental or modeling techniques, the level of effectiveness and optimum glove properties for better performance remains unclear. To fill this gap, hand–arm system dynamics with and without gloves are studied analytically in this work. In this work, we use a lumped parameter model of the hand–arm system, with hand–tool interaction modeled as a linear spring–damper system. The resulting governing equations of motion are solved analytically using the method of harmonic balance. Parametric analysis is performed on the biomechanical model of the hand–arm system with and without a glove to identify key design parameters. It is observed that the effect of glove parameters on its performance is not repetitive and changes in the studied different frequency ranges. This observation further motivates us to optimize the glove parameters to minimize the overall transmissibility in different frequency ranges. [DOI: 10.1115/1.4051662]

Introduction

It is a well-known fact that the prolonged exposure of vibrations to the human body is hazardous and needs to be avoided [1–4]. These unwanted vibrations can be broadly classified into two categories: (1) whole-body vibration (WBV), i.e., vibrations transmitted to the whole body through a vibrating supporting surface, and (2) segmental vibration, i.e., vibrations transmitted to a particular part of the body [5]. Since the measurements and the prolonged effects of WBV (such as spinal disorders, Hemorrhoids, and digestive problems) [6–8] are different from those of segmental vibrations (such as white fingers, muscle injuries, and joint disorders) [2,9], they need to be studied and analyzed separately. Note that WBV has already been studied extensively by researchers across the world. Accordingly, the solutions to minimize the levels of WBV (such as passive air suspension and active electromagnetic suspension) have been well-developed and understood [6–8,10,11]. However, an effective method to reduce the level of segmental vibration still needs to be explored. One of the types of segmental vibrations is hand–arm vibration (HAV), which causes hand–arm vibration syndrome (HAVS). HAVS further includes neurological disorders, vascular, and musculoskeletal injuries. Therefore, it is necessary to understand the dynamics of HAV and accordingly develop methods to minimize it. This is the prime focus of this paper.

Hand–arm vibration syndrome is caused by the vibration transmitted to the human hand through power hand tools used in different sectors such as mining, agriculture, construction, and manufacturing industry. As mentioned earlier, when no preventive measures are taken, HAVS can lead to neurological disorders, vascular and musculoskeletal injuries [12–15]. It has been found that these vascular injuries in the worker's hand will eventually lead to "white fingers," similar to the aging process [16]. Note that HAVS is not limited to the workers in the mining or construction industry only. Prolonged exposure of vibration through daily equipment such as electric grass trimmer also subjects the user to risks of HAVS [17]. Another primary source of HAVS is vibrating steering wheels [2,9,18]. Experimental works have demonstrated that low-frequency vibrations (<40 Hz) are more harmful to drivers of an off-road vehicle [9,19]. Hence, it is required to take preventive measures to limit the levels of HAV.

One of the simple and convenient ways to minimize HAV is the use of antivibration (AV) gloves. Over the last two decades, considerable efforts have been made to measure the effectiveness of AV gloves [20–25]. It has been observed that at high frequencies, the transmissibility of an AV glove increases with increasing glove dynamic stiffness [23] but decreases with increasing apparent mass of the part of the body in contact with the glove material [24]. Also, depending on the glove material, the transmission of vibration through a glove can be increased or decreased when increasing the grip force [25]. However, these AV gloves have shown excellent performance at high frequencies (i.e., >150 Hz), but the inferior performance at low frequencies [26,27]. These observations further motivate us to perform a systematic analysis of hand–tool interaction to understand the dynamics of the hand–arm system with and without gloves and to measure the effectiveness of AV gloves.

To understand the dynamics of HAV with and without AV gloves, different mathematical models have been developed for simulating the biodynamics of the hand–arm system (HAS) (distributed at the finger, palm of hands, and the upper arms) under vibrations. These models are generally presented by multidegree-of-freedom (MDOF) systems with hand–tool interaction modeled as a linear spring–mass–damper system [28–31]. Using these MDOF models for the hand–arm system, it was observed that the transmissibility of the system depends on the body posture, excitation magnitude, and combination of grip and push forces [31]. However, to the best of our knowledge, most of these studies are based on experimental and modeling techniques aimed at determining the effectiveness of the AV glove [26,32–34]. Also, none of the earlier works have systematically analyzed the optimum values of the glove material properties (viz., stiffness, mass, and damping). Hence, this work aims to analytically study the dynamic interactions between a gloved hand–arm and vibrating handle system and determine the optimum values of the AV glove to limit/minimize the transmissibility of HAV.

Toward realizing this goal, we have extended the existing MDOF models of the hand–arm system by including a linear isolator between the source of excitation and handle. This work is an extension of our preliminary work presented for the first time at the 2019 DSCC conference [35]. For the sake of simplicity, the hand–tool interactions are modeled through linear springs and viscous dampers, and accordingly the linear governing equations of motion are presented. The harmonic balance method is used to

[1]Corresponding author.

Manuscript received February 9, 2021; final manuscript received June 26, 2021; published online July 27, 2021. Assoc. Editor: Spencer P. Lake.

analytically study the dynamic of the gloved hand–arm system in contact with a vibrating handle. Optimum values of the glove parameters are obtained to minimize the glove's transmissibility.

Mathematical Formulation

The schematics of a MDOF model of the hand–arm system, without and with gloves, are shown in Fig. 1. Both HAS models were originally developed by Dong et al. [29]. This model is an extension of the MDOF model studied in Ref. [29]. The schematic of the hand–arm system without an AV glove is shown in Fig. 1(*a*). In this model, the hand is represented by a clamp-like structure with m_f and m_p representing the masses of the fingers and combined palm and wrist bone structures, respectively. m_f and m_p are connected through linear viscous and spring elements (c_1, k_1), representing the visco-elastic properties of carpal and metacarpal bones. The masses of tissues and skin covering the fingers and palm–wrist, which is further in contact with the handle of vibrating equipment, are represented by m_{tf} and m_{tp}, respectively. The tissue masses of the fingers and palm–wrist, i.e., m_{tf} and m_{tp}, are coupled to m_f and m_p, respectively, through linear viscous and spring elements (c_2, k_2) and (c_3, k_3) as shown in Fig. 1. The mass

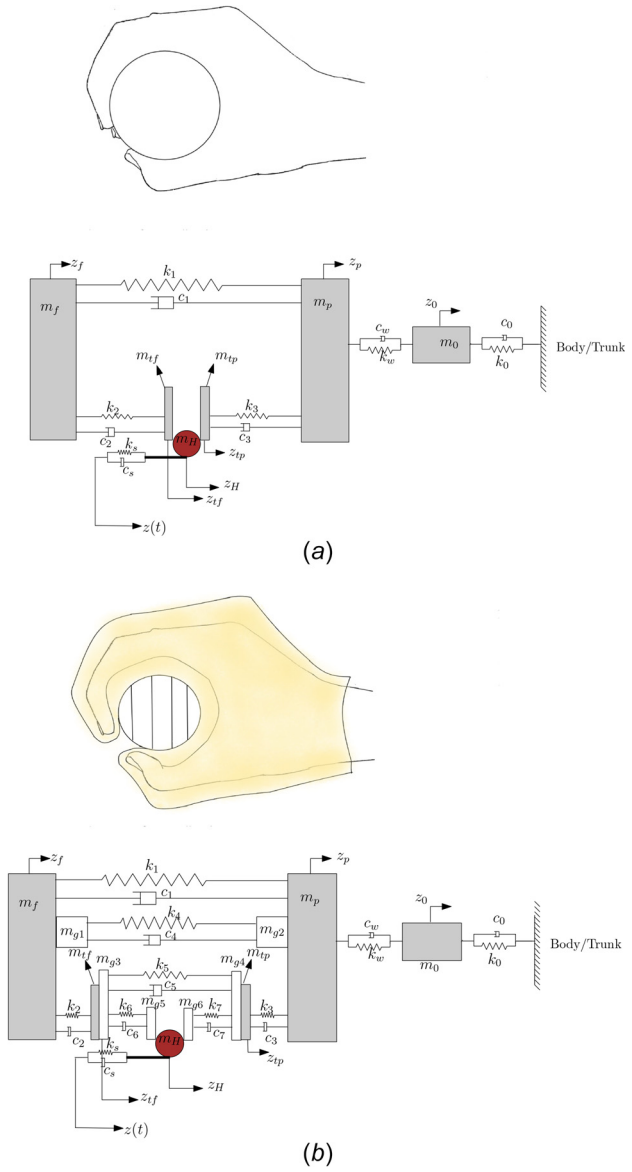

Fig. 1 Schematic of hand–arm system (*a*) without glove and (*b*) with glove coupled to a steering wheel [29]

of the bones, tissues, and the skin of the forearm and upper arm are represented by the lumped mass m_0. Also, the linear viscous-elastic properties of the forearm and upper arm are lumped at the wrist (c_w, k_w). The body/trunk is modeled as a fixed surface and connected to mass m_0 through linear spring and viscous elements $(c_0 \text{ and } k_0)$. The vibrating equipment considered here is a steering wheel connected to the steering box via steering column [36,37]. In this work, vibrations transmitted to the steering box via the engine are modeled as external excitation. Considering the steering column as a rigid bar with a very high stiffness, the visco-elastic properties of the steering column are ignored. Instead, the connection between the steering wheel and steering box is taken to be the visco-elastic property of a rubber cushioning pad between the steering column base and steering box. The handle of the vibrating equipment is modeled as lumped mass m_H, which is in contact with the fingers and palm–wrist. The rubber cushioning pad connecting the handle and the base (which is excited) is modeled with equivalent linear spring (k_s) and viscous damper (c_s). The value of m_H is obtained from Ref. [36], while the values for (k_s) and (c_s) are estimated.

The schematic of the hand–arm system with an AV glove has been shown separately in Fig. 1(*b*). The glove material between the handle and gloved-hand interface is represented by linear viscous (c_6, c_7) and spring elements (k_6, k_7) with lumped mass elements $(m_{g3}, m_{g4}, m_{g5}, m_{g6})$ distributed at the fingers and palm-side interface. The other side of the glove is represented by the additional masses $(m_{g1} \text{ and } m_{g2})$ with linear viscous damper (c_4) and stiffness (k_4) as shown in Fig. 1(*b*). Note that the remaining parameters for this model are the same as the hand–arm system without gloves.

For this analytical model, $z(t)$ is the external excitation. The other generalized coordinates of the hand–arm system with a glove are chosen as the motion of the finger tissue and skin mass m_{tf} (z_{tf}), palm–wrist tissue and skin mass m_{tp} (z_{tp}), fingers mass m_f (z_f), palm–wrist mass m_p (z_p), handle mass m_H (z_H), and lumped forearm and upper-arm mass m_0 (z_0) along the z-direction, making it a 6DOF system. However, it should be noted that for the case of the hand–arm system without a glove z_{tf} and z_{tp} will be the same as z_H, which further makes it a 4DOF model. Having established all the generalized coordinates, we now use the energy method to obtain the equations governing the dynamics for both scenarios.

Case 1: For the case of the hand–arm system without glove (Fig. 1(*a*)), the total kinetic energy (T) and the potential energy (U) of the system are given by

$$T = \frac{1}{2}m_0\dot{z}_0^2 + \frac{1}{2}m_p\dot{z}_p^2 + \frac{1}{2}m_f\dot{z}_f^2 + \frac{1}{2}(m_{\text{tp}} + m_{\text{tf}} + m_H)\dot{z}_H^2 \tag{1a}$$

$$U = \frac{1}{2}k_0z_0^2 + \frac{1}{2}k_w(z_0 - z_p)^2 + \frac{1}{2}k_1(z_p - z_f)^2 + \frac{1}{2}k_2(z_H - z_f)^2 + \frac{1}{2}k_3(z_p - z_H)^2 + \frac{1}{2}k_s(z_H - z)^2 \tag{1b}$$

Accordingly, the Lagrange function for this system is defined as

$$L = T - U \tag{2}$$

and the equations governing the dynamics of the system with time can be obtained from the Euler–Lagrange equation

$$\frac{d}{dt}\left(\frac{\partial L}{\partial \dot{z}_i}\right) - \frac{\partial L}{\partial z_i} = F_i \tag{3}$$

where $z_i's$ are the generalized coordinates, and F_i represents the force in z_i coordinate. These generalized coordinates for the hand–arm system without gloves are $\{\mathbf{z}\} = [z_0, z_f, z_p, z_H]'$. The forces in the generalized coordinates can be written as

$$\begin{bmatrix} F_1 \\ F_2 \\ F_3 \\ F_4 \end{bmatrix} = \begin{bmatrix} -c_0\dot{z}_0 - c_w(\dot{z}_0 - \dot{z}_p) \\ -c_1(\dot{z}_f - \dot{z}_p) - c_2(\dot{z}_f - \dot{z}_H) \\ -c_w(\dot{z}_p - \dot{z}_0) - c_1(\dot{z}_p - \dot{z}_f) - c_3(\dot{z}_p - \dot{z}_H) \\ -c_2(\dot{z}_H - \dot{z}_f) - c_3(\dot{z}_H - \dot{z}_p) - c_s\dot{z}_H + k_s z + c_s\dot{z} \end{bmatrix} \tag{4}$$

Therefore, the equations of motion for the system in these coordinates can be obtained using Eqs. (1)–(3) and can be written in compact form as

$$[\mathbf{M}]\{\ddot{\mathbf{z}}\} + [\mathbf{C}]\{\dot{\mathbf{z}}\} + [\mathbf{K}]\{\mathbf{z}\} = \{\mathbf{F}_{\text{eq}}\} \tag{5}$$

where $[\mathbf{M}]$, $[\mathbf{C}]$, and $[\mathbf{K}]$ are (4×4) inertia, damping, and stiffness matrices, respectively, $\{\mathbf{F}_{\text{eq}}\}$ is (4×1) force vector, and $\{\mathbf{z}\}$ is (4×1) generalized displacement coordinate vector. These matrices are defined in the Appendix. In a next step, we present the equations of motion governing the dynamics of the hand–arm system with gloves.

Case 2: The total kinetic energy and the potential energy of the hand–arm system with gloves are given as

$$\begin{aligned} T_1 = {} & \frac{1}{2}m_0\dot{z}_0^2 + \frac{1}{2}(m_p + m_{g2})\dot{z}_p^2 + \frac{1}{2}(m_f + m_{g1})\dot{z}_f^2 \\ & + \frac{1}{2}(m_{\text{tp}} + m_{g4})\dot{z}_{\text{tp}}^2 + \frac{1}{2}(m_{\text{tf}} + m_{g3})\dot{z}_{\text{tf}}^2 \\ & + \frac{1}{2}(m_{g5} + m_{g6} + m_H)\dot{z}_H^2 \end{aligned} \tag{6a}$$

$$\begin{aligned} U_1 = {} & \frac{1}{2}k_0 z_0^2 + \frac{1}{2}k_w(z_0 - z_p)^2 + \frac{1}{2}k_1(z_p - z_f)^2 + \frac{1}{2}k_2(z_{\text{tf}} - z_f)^2 \\ & + \frac{1}{2}k_3(z_p - z_{\text{tp}})^2 + \frac{1}{2}k_4(z_p - z_f)^2 + \frac{1}{2}k_5(z_{\text{tp}} - z_{\text{tf}})^2 \\ & + \frac{1}{2}k_6(z_H - z_{\text{tf}})^2 + \frac{1}{2}k_7(z_{\text{tp}} - z_H)^2 + \frac{1}{2}k_s(z_H - z)^2 \end{aligned} \tag{6b}$$

Accordingly, the Lagrange function for this system is defined as

$$L_1 = T_1 - U_1 \tag{7}$$

and therefore, the Euler–Lagrange equation for this system will be

$$\frac{d}{dt}\left(\frac{\partial L_1}{\partial \dot{\hat{z}}_i}\right) - \frac{\partial L_1}{\partial \hat{z}_i} = \hat{F}_i \tag{8}$$

where $\hat{z}_i$ are generalized coordinates of the system with gloves, and $\hat{F}_i$ represents the force in $\hat{z}_i$ coordinate. The generalized coordinates for the hand–arm system with gloves will be $\{\hat{\mathbf{z}}\} = [z_0, z_f, z_p, z_{\text{tp}}, z_{\text{tf}}, z_H]'$. The forces in the generalized coordinates can be written as

$$\begin{bmatrix} \hat{F}_1 \\ \hat{F}_2 \\ \hat{F}_3 \\ \hat{F}_4 \\ \hat{F}_5 \\ \hat{F}_6 \end{bmatrix} = \begin{bmatrix} -c_0\dot{z}_0 - c_w(\dot{z}_0 - \dot{z}_p) \\ -(c_1 + c_4)(\dot{z}_f - \dot{z}_p) - c_2(\dot{z}_f - \dot{z}_{\text{tf}}) \\ -(c_1 + c_4)(\dot{z}_p - \dot{z}_f) - c_3(\dot{z}_p - \dot{z}_{\text{tp}}) - c_w(\dot{z}_p - \dot{z}_0) \\ -c_5(\dot{z}_{\text{tp}} - \dot{z}_{\text{tf}}) - c_3(\dot{z}_{\text{tp}} - \dot{z}_p) - c_7(\dot{z}_{\text{tp}} - \dot{z}_H) \\ -c_5(\dot{z}_{\text{tf}} - \dot{z}_{\text{tp}}) - c_2(\dot{z}_{\text{tf}} - \dot{z}_f) - c_6(\dot{z}_{\text{tf}} - \dot{z}_H) \\ -c_6(\dot{z}_H - \dot{z}_{\text{tf}}) - c_7(\dot{z}_H - \dot{z}_{\text{tp}}) - c_s\dot{z}_H + k_s z + c_s\dot{z} \end{bmatrix} \tag{9}$$

Hence, the equations of motion for the hand–arm system with glove in these coordinates can be obtained using Eqs. (6)–(8) and can be written in a compact form as

$$[\mathbf{M}_1]\{\ddot{\hat{\mathbf{z}}}\} + [\mathbf{C}_1]\{\dot{\hat{\mathbf{z}}}\} + [\mathbf{K}_1]\{\hat{\mathbf{z}}\} = \left\{\hat{\mathbf{F}}_{\text{eq}}\right\} \tag{10}$$

where $[\mathbf{M}_1]$, $[\mathbf{C}_1]$, and $[\mathbf{K}_1]$ are (6×6) inertia, damping, and stiffness matrices, respectively, $\left\{\hat{\mathbf{F}}_{\text{eq}}\right\}$ is (6×1) force vector, and $\{\hat{\mathbf{z}}\}$ is (6×1) generalized displacement coordinate vector. These matrices are further defined in the Appendix.

Experimental Validation of Hand–Arm System Model

To ensure that the response of the HAS model with and without a glove (described in the "Mathematical Formulation" section) matches with the response of a real human HAS, we compare the HAS model's response at the palm and finger against the experimental results measured at the palm and finger of a human being. To perform this comparison, we use unweighted relative transmissibility as defined below:

$$\begin{aligned} (t_p)_{\text{without glove}} &= \frac{z_p}{Z_0} \\ (t_f)_{\text{without glove}} &= \frac{z_f}{Z_0} \end{aligned} \tag{11}$$

Similarly, the unweighted transmissibilities of the palm and fingers with a glove are defined as

$$\begin{aligned} (t_p)_{\text{with glove}} &= \frac{(z_p)_{\text{with glove}}}{Z_0} \\ (t_f)_{\text{with glove}} &= \frac{(z_f)_{\text{with glove}}}{Z_0} \end{aligned} \tag{12}$$

Then, the "relative transmissibilities" at the palm and fingers [29] are defined as

$$\begin{aligned} T_p &= \frac{(t_p)_{\text{with glove}}}{(t_p)_{\text{without glove}}} \\ T_f &= \frac{(t_f)_{\text{with glove}}}{(t_f)_{\text{without glove}}} \end{aligned} \tag{13}$$

The parameters used for this part of the exercise correspond to a gel-filled glove as reported by Dong et al. [29]. To obtain the models' relative transmissibility response, the numerical time response of the system to broadband random excitation, with a flat power spectral density of $3.0\,(\text{m/s}^2)^2/\text{Hz}$, is obtained using MATLAB routine "ode45." Afterwards, the system's frequency response is obtained using the fast Fourier transform on the time response, which is obtained using the MATLAB built-in command "fft." Further, the experimental transmissibility data at the palm are obtained using the palm adapter method [28], while the experimental transmissibility data at the finger are obtained using the experimental biodynamic method [29].

The comparison between the experimental and model response data against each other is shown in Fig. 2. From Fig. 2, the experimental data and model responses match with a few discrepancies as also noted in Ref. [29]. For the finger response, the modeled transmissibility values deviate from the experimental transmissibility values at frequencies less than 100 Hz. Apart from these deviations, the response of the model is fairly consistent with the response obtained experimentally. As such, we proceed using the model responses to analyze the AV glove.

The analytical solutions of these coupled second-order ordinary differential equations for the hand–arm system with and without gloves (Eqs. (5) and (10)) are presented in the Analytical Solution section.

Analytical Solution

In this section, we briefly present the method of harmonic balance (i.e., undetermined coefficient method) to solve the equations

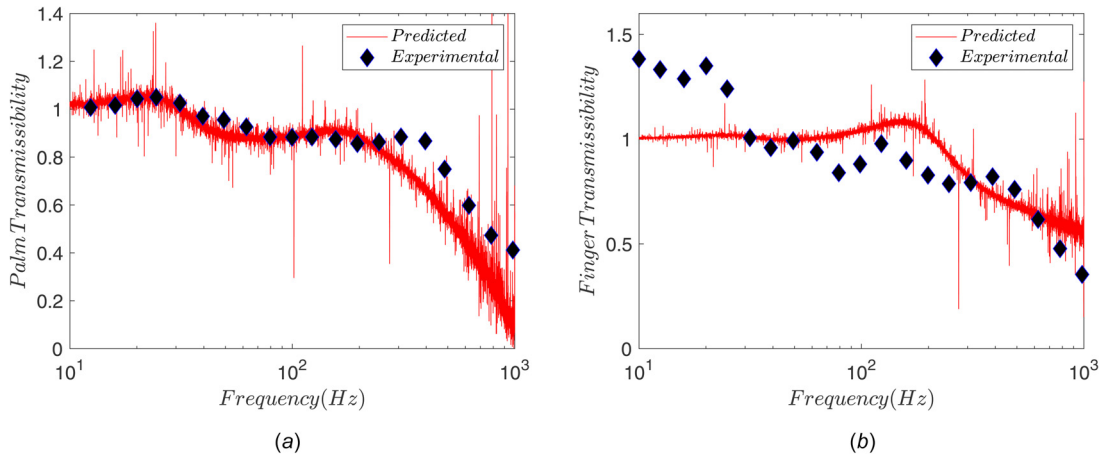

Fig. 2 Comparison of the HAS model relative transmissibility response with experimental transmissibility response at the (*a*) palm and at the (*b*) finger

of motion governing the dynamics of the hand–arm system with and without gloves. For the current analysis, we employ a harmonic excitation in the form of

$$z(t) = Z_0 \cos(\omega t) \tag{14}$$

where Z_0 and ω are the amplitude and frequency of the external excitation, respectively. At this stage, we look for the solutions synchronous with external excitation, and hence, without any loss of generality, we assume the solutions of Eqs. (5) and (10) in the form of

$$\{\mathbf{z}\}(t) = \{\mathbf{A}\}\cos(\omega t) + \{\mathbf{B}\}\sin(\omega t) \tag{15}$$

$$\{\hat{\mathbf{z}}\}(t) = \{\mathbf{A}_1\}\cos(\omega t) + \{\mathbf{B}_1\}\sin(\omega t) \tag{16}$$

where $\{\mathbf{A}\}$ and $\{\mathbf{B}\}$ are (4×1) columns vectors with unknown coefficients $A_i's$ and $B_i's$ $(i = 1 - 4)$, respectively, and $\{\mathbf{A}_1\}$ and

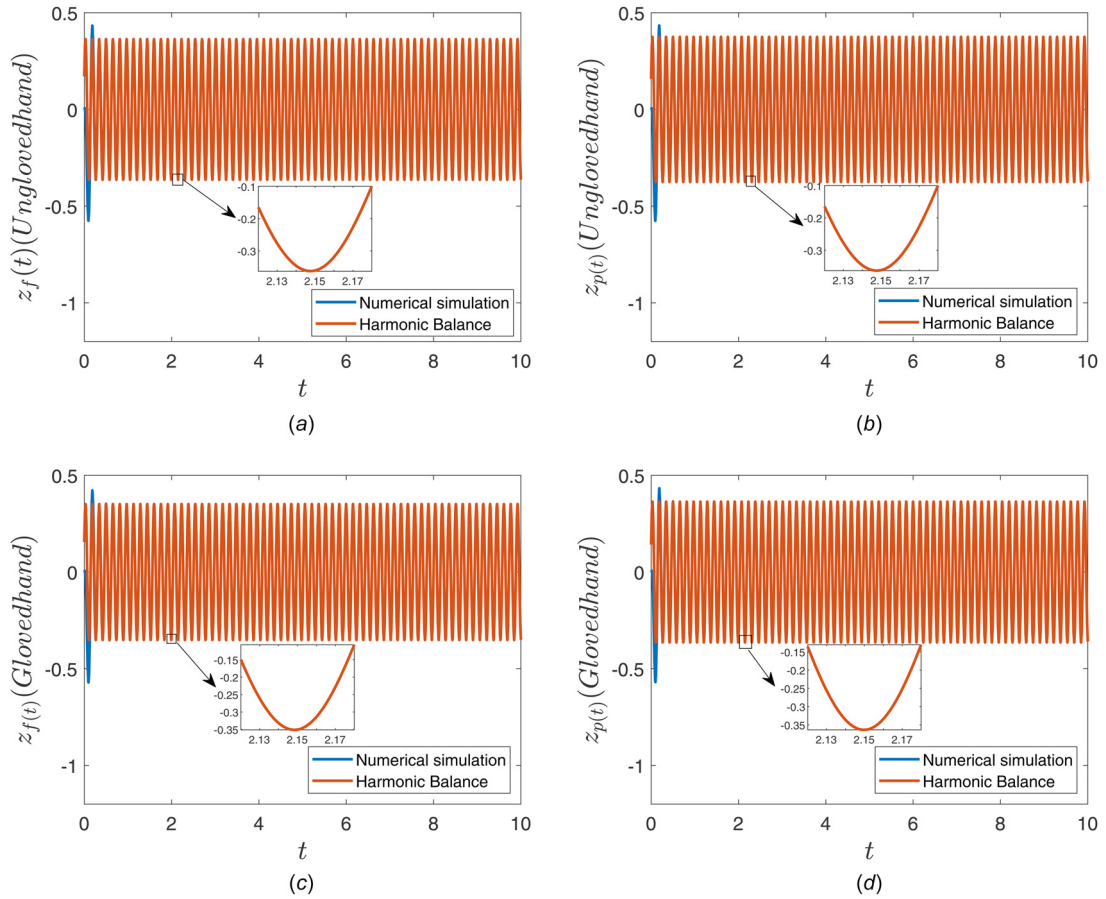

Fig. 3 Comparison of numerical and analytical solutions for the responses of (*a*) fingers without gloves, (*b*) palm without gloves, (*c*) fingers with gloves, and (*d*) palm with gloves. The other parameters are chosen as $Z_0 = 1$, $\omega = 40$ rad/s, $m_{g2} = m_{g1}$, $m_{g4} = m_{g3}$, $m_{g6} = m_{g5}$, $k_7 = k_6$, and $c_7 = c_6$.

$\{\mathbf{B}_1\}$ are (6×1) columns vectors with unknown coefficients $A'_{1i}s$ and $B'_{1i}s$ $(i = 1 - 6)$, respectively. On substituting $\{\mathbf{z}\}(t)$ and $\{\hat{\mathbf{z}}\}(t)$ in Eqs. (5) and (10), respectively, we get

$$\begin{aligned} &-\omega^2[\mathbf{M}]\{\mathbf{A}\}\cos(\omega t) - \omega^2[\mathbf{M}]\{\mathbf{B}\}\sin(\omega t) \\ &-\omega[\mathbf{C}]\{\mathbf{A}\}\sin(\omega t) + \omega[\mathbf{C}]\{\mathbf{B}\}\cos(\omega t) + [\mathbf{K}]\{\mathbf{A}\}\cos(\omega t) \\ &+[\mathbf{K}]\{\mathbf{B}\}\sin(\omega t) = \{\mathbf{F}_{\text{eq}}\} \end{aligned} \tag{17}$$

$$\begin{aligned} &-\omega^2[\mathbf{M}_1]\{\mathbf{A}_1\}\cos(\omega t) - \omega^2[\mathbf{M}_1]\{\mathbf{B}_1\}\sin(\omega t) \\ &-\omega[\mathbf{C}_1]\{\mathbf{A}_1\}\sin(\omega t) + \omega[\mathbf{C}_1]\{\mathbf{B}_1\}\cos(\omega t) \\ &+[\mathbf{K}_1]\{\mathbf{A}_1\}\cos(\omega t) + [\mathbf{K}_1]\{\mathbf{B}_1\}\sin(\omega t) = \left\{\hat{\mathbf{F}}_{\text{eq}}\right\} \end{aligned} \tag{18}$$

By equating the coefficients of sine and cosine on both sides of Eqs. (17) and (18), we obtain two sets of algebraic equations corresponding to the ungloved and gloved hand, respectively. On solving these linear algebraic equations, we get $\{\mathbf{A}\}$, $\{\mathbf{B}\}$, $\{\mathbf{A1}\}$, and $\{\mathbf{B1}\}$, and accordingly, the amplitude vectors $\{\mathbf{z}\}$ and $\{\hat{\mathbf{z}}\}$ (Eqs. (15) and (16)). The closed-form expressions of the elements of these amplitude vectors are very complex and hence, for the sake of brevity, are not reported. A detailed analysis of the systems, i.e., HAS with and without gloves, using the analytical solutions is presented in the Results and Discussion section.

Results and Discussion

In this section, a parametric study is carried out to analyze the effectiveness of the antivibration gloves against the transmitted vibrations. The mechanical properties of the hand–arm system and glove, used for the numerical simulations, are presented in Table 1. For the sake of simplicity in the parametric analysis, the

Table 1 Parameters of the hand–arm system and glove based on parameters of a gel-filled glove determined in Ref. [29]

Parameter	Value	Units	Parameter	Value	Units	Parameter	Value	Units
m_0	6.015	(kg)	k_0	7567	N/m	c_0	106	N s/m
m_p	1.4618	(kg)	k_w	2978	N/m	c_w	134	N s/m
m_f	0.0958	(kg)	k_1	4221	N/m	c_1	52	N s/m
m_{tp}	0.0338	(kg)	k_2	196,038	N/m	c_2	122	N s/m
m_{tf}	0.0186	(kg)	k_3	55,564	N/m	c_3	126	N s/m
m_{g1}	0.0674	(kg)	k_4	2417	N/m	c_4	1	N s/m
m_{g3}	0.0651	(kg)	k_5	0	N/m	c_5	0	N s/m
m_{g5}	0.0005	(kg)	k_6	454,779	N/m	c_6	106	N s/m
m_H	3	(kg)	k_s	940	N/m	c_s	79	N s/m

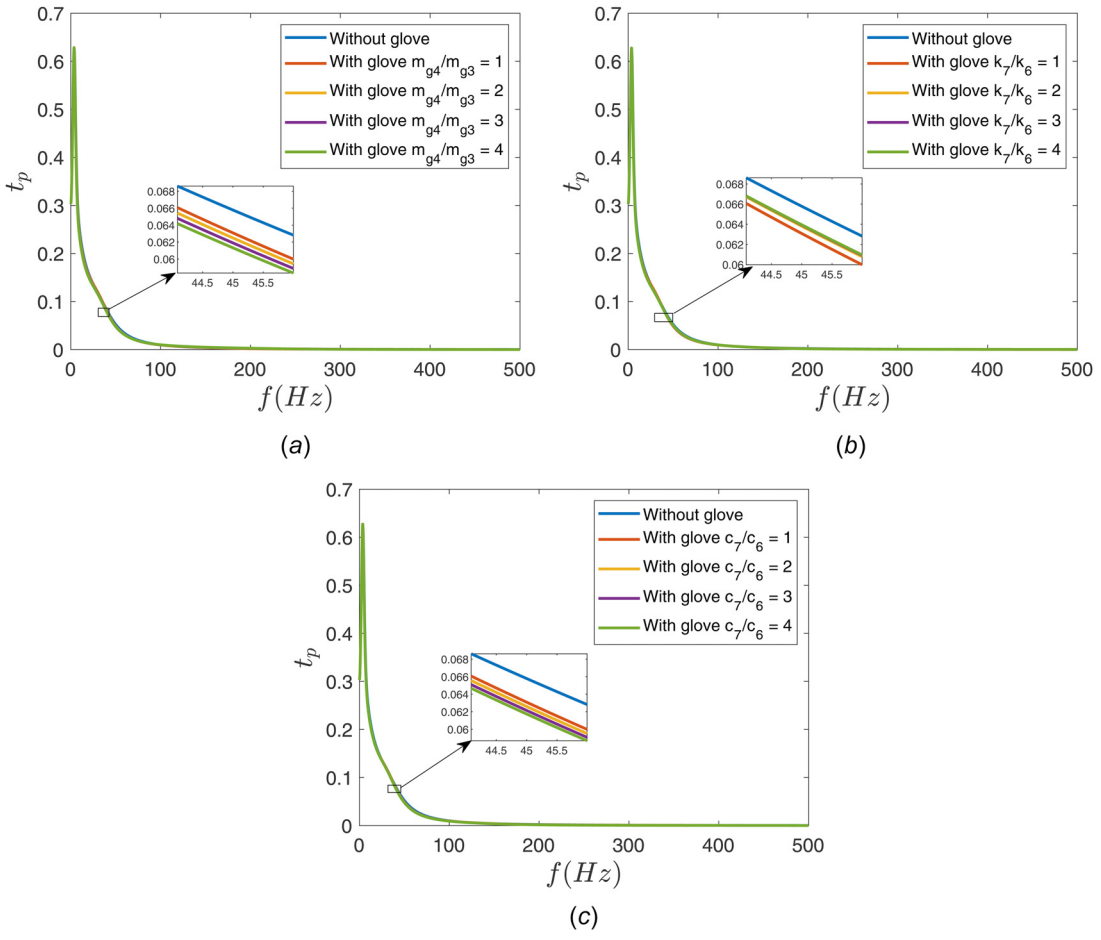

Fig. 4 Comparison of palm transmissibility curves with and without gloves with different glove parameters

numerical values of m_{g2}, m_{g4}, m_{g6}, k_7, and c_7 are kept proportional to m_{g1}, m_{g3}, m_{g5}, k_6, and c_6, respectively.

The first part of the analysis is to validate the obtained analytical solutions by comparing them against the numerical simulations of Eqs. (5) and (10). The comparison between numerical solutions from Eqs. (5) and (10) and analytical solutions from Eqs. (15) and (16) is presented for $m_{g2} = m_{g1}$, $m_{g4} = m_{g3}$, $m_{g6} = m_{g5}$, $k_7 = k_6$, and $c_7 = c_6$. The initial conditions for numerical simulations are chosen corresponding to steady-state response. For the numerical simulations of Eqs. (5) and (10), we have used the built-in command ode45 in MATLAB with very tight absolute tolerance and relative tolerance (1×10^{-10}).

To compare the analytical solutions and numerical simulations, we have used the responses of palm and finger (z_p and z_f) and are shown in Fig. 3. Figures 3(*a*) and 3(*b*) represent the responses of the fingers and palm without gloves, respectively, while Figs. 3(*c*) and 3(*d*) represent the responses of the fingers and palm with gloves, respectively. From Fig. 3, we can observe that there is an excellent agreement between the numerical simulations and analytical solutions for the given values of system parameters. This agreement further improves with the increase in time steps. Therefore, in the remainder of this work, we use the analytical solutions for the analysis. Having obtained the solution for the response of different parts of the hand–arm system, the effect of different glove parameters on the unweighted glove transmissibility (as defined in Eqs. (11) and (12)) is shown.

For the sake of brevity, we present the transmissibility response for the palm only. The comparison of palm's transmissibility with and without an AV glove for different glove parameters has been shown in Fig. 4. In this figure, the peak value of the curve represents the instance of primary resonance. However, the frequency corresponding to the second and third resonance is not evident. From Fig. 4, it also seems that the transmissibility response of the palm with the glove is almost similar to the one without the glove and is independent of the glove's parameters.

To make these figures easier to read, the transmissibility data, with different masses of the AV gloves, are displayed on a log–log scale. As can be seen from Fig. 5(*a*), the first resonance peak is evident, while the appearance of the second resonance peak is slightly apparent. However, similar to the data presented on a linear scale (Fig. 4), it is difficult to observe the impact of different masses of the glove on the transmissibility at the palm on log scale. To make sure this phenomenon was not unique to the palm, the parametric study analyzing the effects of the glove's mass was also performed while examining transmissibility at the fingers. As seen from Fig. 5(*b*), it is almost impossible to distinguish between the transmissibility plots for different masses of the AV glove, even though the appearance of resonance peaks on the transmissibility plot is more apparent. Therefore, to have a better understanding of the effectiveness of the AV glove and role of different glove parameters, we use the relative transmissibility (as defined in Eq. (13)).

The effect of different glove parameters on the relative transmissibilities is depicted in Fig. 6. From these figures, we observe that the instances of the primary and secondary resonances are more evident in relative transmissibility than in absolute transmissibility. Also, the effect of the glove parameters on the glove's performance is clearly visible through relative transmissibility. For instance, the masses of the glove in direct contact with the handle do not influence the transmissibility significantly. However, the other glove parameters, which are in direct contact with the hand, significantly influence the performance of the glove. From Fig. 6, we can observe that the effect of different glove parameters on the relative transmissibility is not uniform over a wide frequency range, in our case 0–500 Hz. Therefore, it is not possible to select global key parameters of glove, which can enhance the performance of AV glove over a wide frequency range. Instead depending on the excitation frequency, key design parameters of glove can decided to enhance the performance.

It is a well-established fact that damping in some dynamical systems plays a vital role in achieving better transmissibility [38]. Therefore, it is necessary to have a better understanding of the effects of damping properties of different parts of gloves on its performance. To assess the effect of damping on the performance of an AV glove, we compare relative finger and palm transmissibilities corresponding to the excitation frequencies in the amplification (f_A) and isolation zones (f_I) with varying values of damping parameters of the AV glove. Excitation frequencies in the isolation region of either the palm or finger satisfy the relation

$$\frac{\omega_{\text{excitation}}}{\omega_{\text{natural frequency,finger/palm}}} > \sqrt{2}$$

while excitation frequencies in the amplification region of either the palm or finger satisfy the relation

$$\frac{\omega_{\text{excitation}}}{\omega_{\text{natural frequency,finger/palm}}} < \sqrt{2}$$

The amplification region of the fingers and palm corresponds to the excitation frequencies below 322 Hz and 43 Hz, respectively. Similarly, the isolation region of the fingers and palm corresponds to the excitation frequencies above 322 Hz and 43 Hz, respectively.

Figure 7 depicts the variation of the relative finger transmissibilities, for f_A and f_I, with different damping properties of the

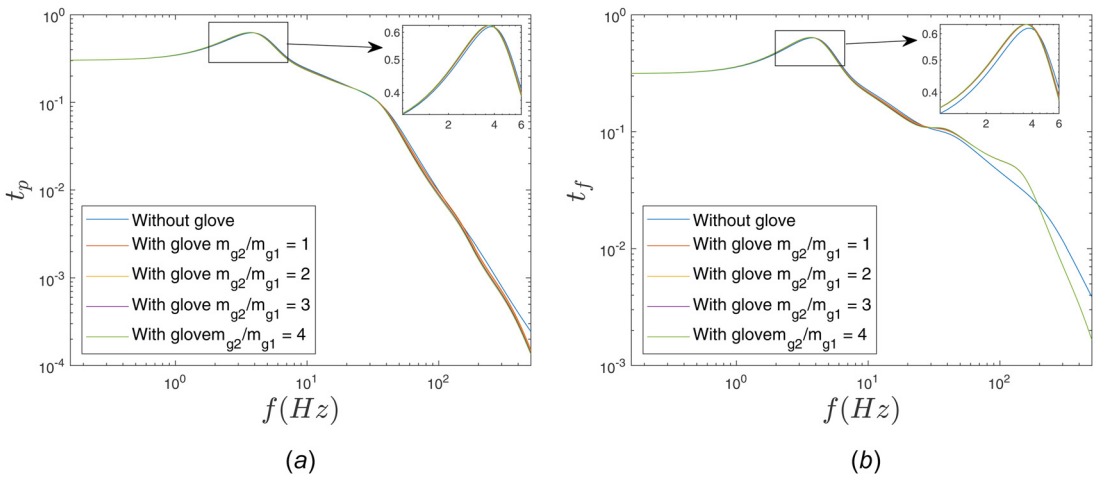

Fig. 5 Comparison of palm and finger transmissibility curves with and without gloves with different glove parameters on axes with logarithm scales

glove. From Fig. 7(*a*), we can observe that with an increase in c_4, the relative transmissibility decreases irrespective of the excitation frequencies. However, this observation does not hold any longer for the case of c_6 and c_7. From Fig. 7(*b*), we observe that the relative transmissibility first decreases with an increase in the value of c_6 and reaches a minimum value at c_6^*. With a further increase in c_6 after c_6^*, the relative transmissibility starts increasing again and asymptotically reaches a constant value. A similar observation can be drawn for the case of c_7 also, i.e., with an increase in c_7, the relative transmissibility decreases and asymptotically reaches a constant value.

Further, we observe that the relative finger transmissibility corresponding to f_I always remains lower than the transmissibility corresponding to f_A irrespective of the value of c_6 and c_7. This further implies that the choices of c_6 and c_7 for better isolation are independent of amplification and isolation zones. However, this observation does not hold any longer for the case of c_4. As the value of c_4 increases, the relative finger transmissibility corresponding to f_A becomes lower than the transmissibility corresponding to f_I after a critical value of $c_4(c_4^*)$. However, with a further increase in c_4, the relative finger transmissibility corresponding to f_A again becomes more significant than the transmissibility corresponding to f_I. These observations further help in

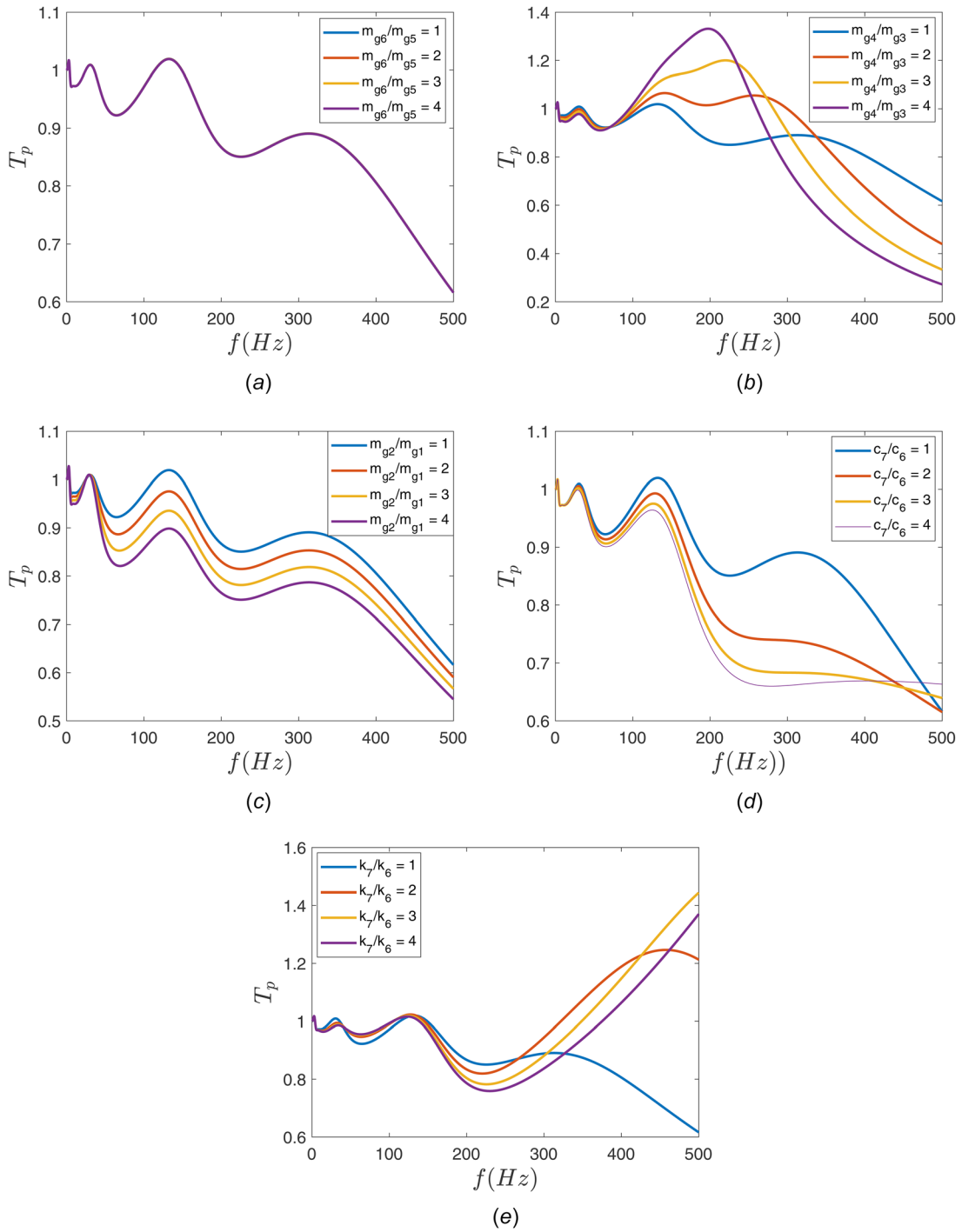

Fig. 6 Comparison of relative palm transmissibility curves with different glove parameters

deciding the ranges of damping parameters to get better vibration isolation for the fingers.

Now, we look for the effects of different damping parameters on the relative palm transmissibility. From Fig. 8(*a*), we observe that only low values of c_4 provide better isolation at the palm for the excitation frequency corresponding to the amplification zone. However, this observation is not valid for the case of excitation frequency in the isolation zone. Figure 8(*c*) shows that with an increase in c_7 the transmissibility of the palm decreases to a minimum value at c_7^* after which it increases again and asymptotically reaches a constant value. Further, we observe that c_6 has no significant effect on the performance of AV glove for the vibration isolation of palm (Fig. 8(*b*)).

These observations further help to guide the way various parameters in an antivibration glove are tuned, thus ensuring maximum vibration attenuation at a specific frequency, at which they may be employed. Also, we observe that the effect of the parameters studied on the performance of glove is not monotonous and changes from one frequency to another frequency. This observation is in consistency with earlier findings that the performance/effectiveness of the AV glove significantly depends on the application and, consequently, on the frequency of the external excitation.

With this motivation, we optimize the glove parameters to minimize the overall transmissibility, and this is presented in the Optimization of Glove Parameters section.

Optimization of Glove Parameters

In this section, we present the optimization of glove parameters for better isolation performance. Since palm and fingers are in direct contact with the vibrating steering wheel. We optimize glove parameters to minimize both, i.e., palm and finger relative transmissibility together. To perform the multi-objective optimzation, we have used MATLAB's built-in function "gamultiobj." These optimization simulations have been performed with relatively larger number of initial points, more specifically 10^5, to ensure the convergence of glove parameters toward optimum values. gamultiobj returns the value of optimized parameters on the Pareto front of objective functions (set of inferior objective function values in the space of objective functions). Note that it is more beneficial to design a glove with optimal parameters for a specific application rather than for global purpose. On considering this fact, we perform multi-objective optimization for three different frequency ranges; more specifically, antivibration gloves are optimized for a low-frequency (5–25 Hz), medium-frequency (25–200 Hz), and high-frequency (200–1250 Hz) ranges. Further, for the sake of simplicity in the analysis, we consider that properties of steering wheel do not change in these different frequency ranges. Therefore, we are designing the antivibration glove for different vehicles which have varying excitation frequencies due to factors such as road terrain or vehicle type. Even though the optimization results presented in this section are particular to the system with the steering wheel described, the optimization technique employed is meant to be applicable to a wide variety of tools whose mass and visco-elastic properties are different from the vibrating equipment described in this paper.

Before proceeding further, we define weighted palm and finger's transmissibility for optimization. According to the ISO standard 10819 [39], the weighted transmissibilities at the palm and fingers without a glove (wng) are defined as

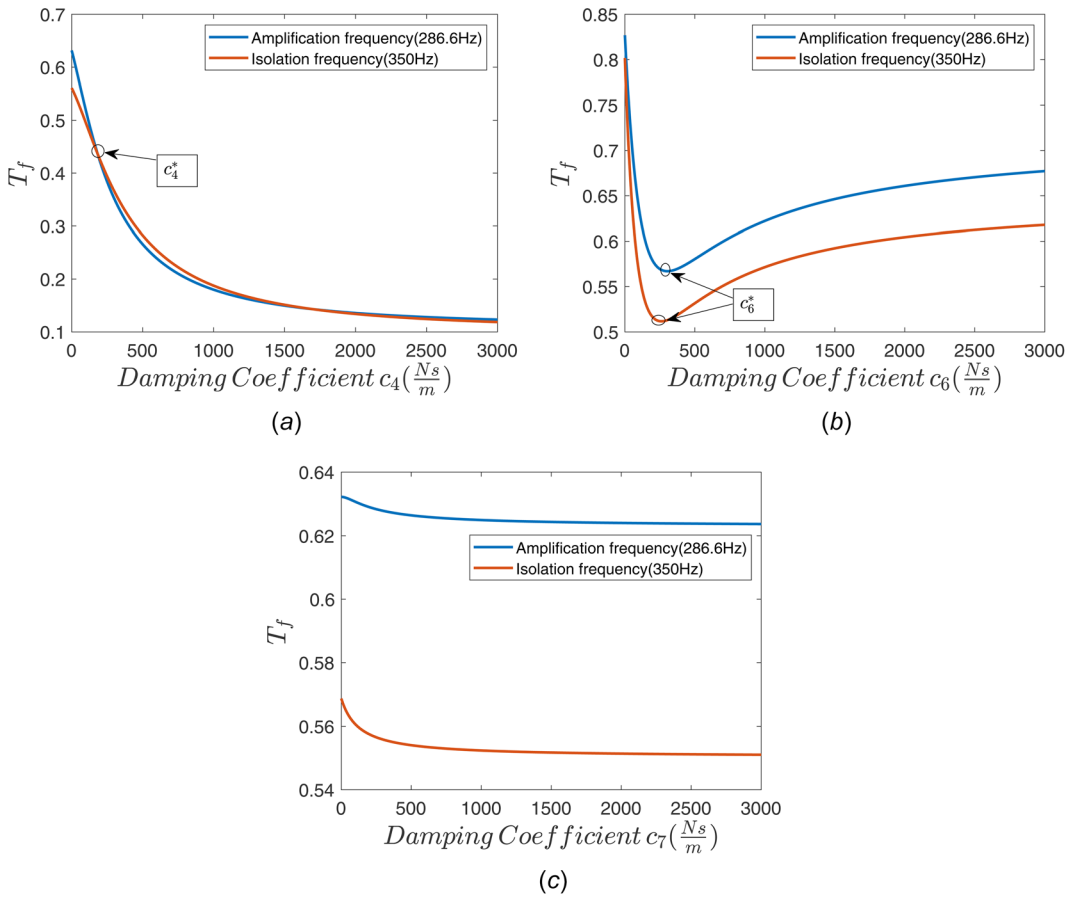

Fig. 7 Comparison of the relative finger transmissibility curves for the frequencies in amplification ($f_A = 286.6$ Hz) and isolation zone ($f_I = 350$ Hz) with different damping values of glove (*a*) connecting finger and palm (c_4), (*b*) connecting handle and finger-tip (c_6), and (*c*) connecting handle and palm-tip (c_6)

$$(t_p)_{\text{wng}} = \frac{\sqrt{\sum_{i=i_L}^{i_u}\left[(z_p)_{\text{without glove}} * \omega_i^2 * W_{hi}\right]^2}}{\sqrt{\sum_{i=i_L}^{i_u}\left[Z_0 * \omega_i^2 * W_{hi}\right]^2}}$$

$$(t_f)_{\text{wng}} = \frac{\sqrt{\sum_{i=i_L}^{i_u}\left[(z_f)_{\text{without glove}} * \omega_i^2 * W_{hi}\right]^2}}{\sqrt{\sum_{i=i_L}^{i_u}\left[Z_0 * \omega_i^2 * W_{hi}\right]^2}} \tag{19}$$

Similarly, the weighted transmissibilities at the palm and fingers with the glove (wg) can be written as

$$(t_p)_{\text{wg}} = \frac{\sqrt{\sum_{i=i_L}^{i_u}\left[(z_p)_{\text{with glove}} * \omega_i^2 * W_{hi}\right]^2}}{\sqrt{\sum_{i=i_L}^{i_u}\left[Z_0 * \omega_i^2 * W_{hi}\right]^2}}$$

$$(t_f)_{\text{wg}} = \frac{\sqrt{\sum_{i=i_L}^{i_u}\left[(z_f)_{\text{with glove}} * \omega_i^2 * W_{hi}\right]^2}}{\sqrt{\sum_{i=i_L}^{i_u}\left[Z_0 * \omega_i^2 * W_{hi}\right]^2}} \tag{20}$$

In these expressions, both i_L and i_u represent one-third-octave frequency band numbers, ω_i is the one-third-octave center frequency for the ith one-third-octave band, and W_{hi} represents the frequency weighting corresponding to each ith band number as shown in ISO 10819. For the low-frequency range, i_L is set to 6 and i_u is set to 14. For the medium-frequency range, i_L is set to 14 and i_u is set to 23. For the high-frequency range, i_L is set to 23 and i_u is set to 31. The values for the frequency weighting for the low-frequency range are obtained from Ref. [40]. Therefore, the relative weighted transmissibilities for the palm and finger, i.e., T_{pw} and T_{pf}, respectively, are defined as

$$T_{\text{pw}} = \frac{(t_p)_{\text{wg}}}{(t_p)_{\text{wng}}} \tag{21}$$

$$T_{\text{fw}} = \frac{(t_f)_{\text{wg}}}{(t_f)_{\text{wng}}} \tag{22}$$

In a next step, we define our objective/fitness function for the gamultiobj as

$$\text{objective function} = \min(T_{\text{pw}}, T_{\text{fw}})$$
$$\{\mathbf{lb}\} \le \{\mathbf{x} \le \{\mathbf{ub}\}$$

where $\{\mathbf{x}\}$ represents the vector containing glove parameters to be optimized and is given by

$$\{\mathbf{x}\} = \{m_{g3}, k_4, k_5, k_6, k_7, c_4, c_5, c_6, c_7\}$$

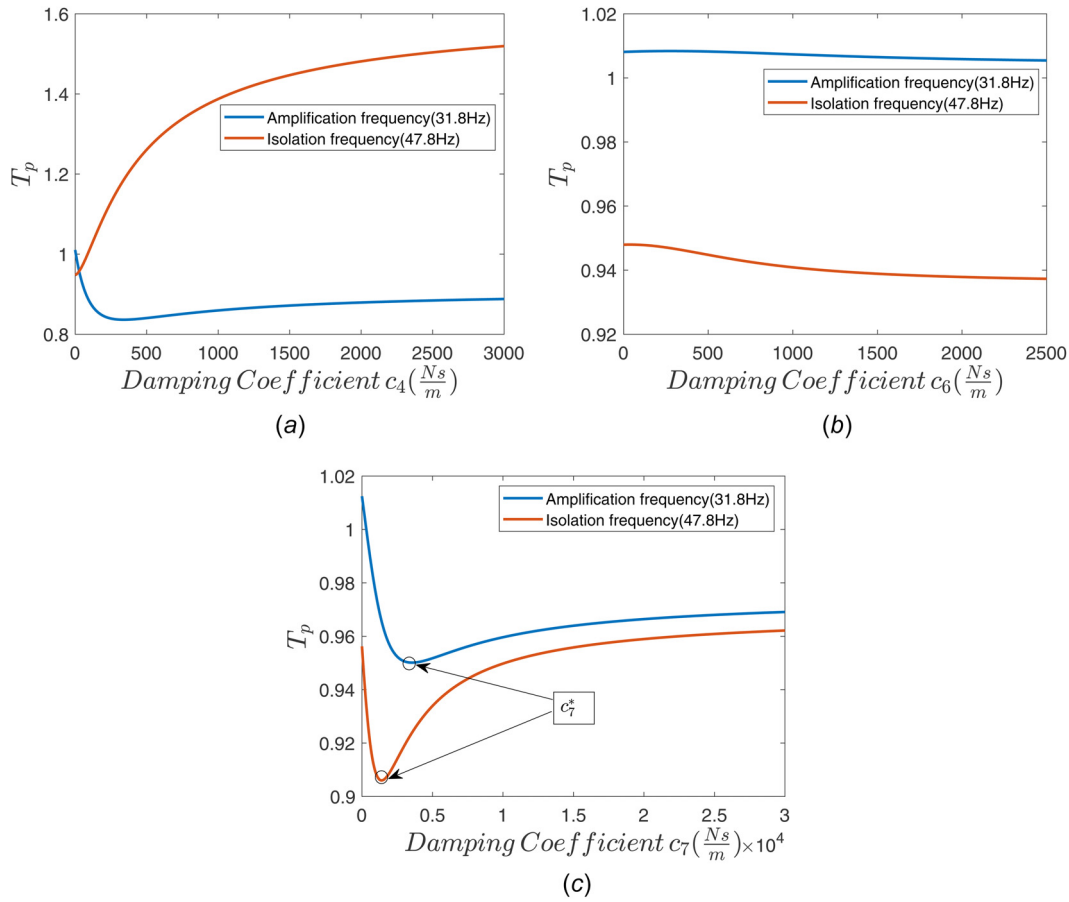

Fig. 8 Comparison of the relative palm transmissibility curves for the frequencies in amplification ($f = 31.8$ Hz) and isolation zone ($f = 47.8$ Hz) with different damping values of glove (*a*) connecting finger and palm (c_4), (*b*) connecting handle and finger-tip (c_6), and (*c*) connecting handle and palm-tip (c_6)

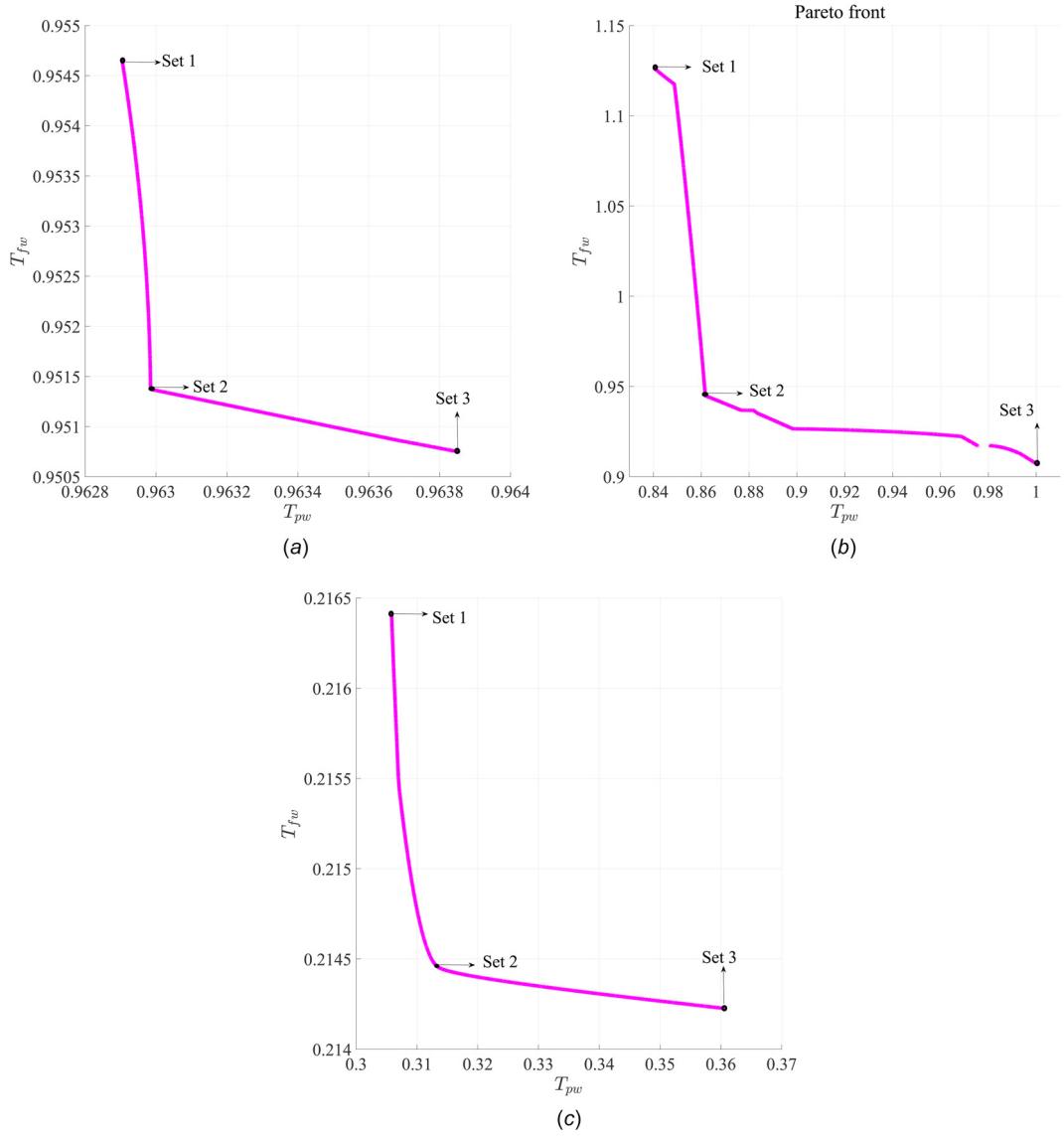

Fig. 9 Pareto front for (*a*) low-frequency range, (*b*) medium-frequency range, and (*c*) high-frequency range

Also, $\{\mathbf{lb}\}$ and $\{\mathbf{ub}\}$ represent the lower and upper bounds of the parameters, respectively, and are given by

$$\{\mathbf{lb}\} = \{0.0001,\ 10^3,\ 10^3,\ 10^5,\ 10^5,\ 0.0001,\ 0.0001,\ 10,\ 10\}$$

and

$$\{\mathbf{ub}\} = \{0.1302,\ 2417,\ 2417,\ 10^6,\ 10^6,\ 1,\ 1,\ 200,\ 200\}$$

These parameters have the same units as the parameters of the glove defined in Table 1. The other parameters of the optimization glove are not changed to avoid adding weight to the antivibration glove. Since antivibration gloves are supposed to be more effective at the fingers, we decided to optimize the glove mass which is in direct contact with fingers, i.e., m_{g3} (Fig. 1). The upper bounds for m_{g3} of the glove are obtained by doubling the value of m_{g3} shown in Table 1. The lower bound for the gloves mass parameter is assumed to be the smallest glove mass (m_{g5}) rounded down to the nearest power of 10.

The upper bounds for the elastic properties of the glove k_6 and k_7 are determined by rounding up their values presented earlier to the nearest power of 10. However, the upper bounds for the viscous properties of the glove c_6 and c_7 are determined by rounding up their value to the nearest multiple of 100. The lower bounds for k_6, k_7, c_6, and c_7 are then determined by rounding down their values from Table 1 to the nearest power of 10.

Furthermore, Wimer et al. [41] observed that the high stiffness of antivibration gloves' elements, connecting the elements of

Table 2 Comparison of optimal parameters obtained from Pareto front for low-frequency range

	m_{g3}	k_4	k_5	k_6	k_7	c_4	c_5	c_6	c_7	T_{pw}	T_{fw}
Set 1	0.1302	1239.34	1771.85	10^6	10^6	1	1	62.67	200	0.9629	0.9547
Set 2	0.1302	2417	1770.89	10^6	10^6	1	1	62.63	200	0.9630	0.9514
Set 3	0.1302	2417	1762.32	10^6	10^6	0	0.0304	135.6	105.92	0.9639	0.9507

Table 3 Comparison of optimal parameters obtained from Pareto front for medium-frequency range

	m_{g3}	k_4	k_5	k_6	k_7	c_4	c_5	c_6	c_7	T_{pw}	T_{fw}
Set 1	0.1302	1053.87	1312.4	9.75×10^5	10^5	1	1	200	200	0.8404	1.1263
Set 2	0.1302	1054.14	1320.45	10^5	10^5	1	1	200	200	0.8617	0.9449
Set 3	0.000105	2327.66	1202.8	10^5	9.65×10^5	1	1	200	198.9721	1.0008	0.9067

Table 4 Comparison of optimal parameters obtained from Pareto front for high-frequency range

	m_{g3}	k_4	k_5	k_6	k_7	c_4	c_5	c_6	c_7	T_{pw}	T_{fw}
Set 1	0.1302	1166.98	1424.9	10^5	10^5	1	1	10	53.78	0.3058	0.2164
Set 2	0.1302	10^3	10^3	10^5	10^5	1	0	16.6	50.58	0.3135	0.2145
Set 3	0.1302	10^3	10^3	10^5	10^5	1	0	17.6544	10.0004	0.3605	0.2142

gloves in direct contact with finger and palm (k_4), causes reduction in the grip strength as compared to grip strength without gloves. This reduction in the grip strength can be compensated by exerting more pressure from human side. However, high values of grip strength during operating a machinery can be detrimental to the operators of the machinery. Therefore, it is required that antivibration gloves are design such that minimal grip strength is exerted while operating a machinery. With the consideration of this observation, the upper bounds of the glove parameters responsible for grip strength, i.e., k_4, k_5, c_4, c_5, were chosen as the respective maximum values of the glove parameters studied in the Results and Discussion section. More specifically, the upper bounds of k_4 and k_5 are chosen as 2417, whereas the upper bounds of c_4 and c_5 are chosen as 1. The lower bounds of the glove properties, k_4 and k_5, were chosen to be the presented values of k_4 and k_5 rounded down to the nearest power of 10, while the lower bounds for c_4 and c_5 were chosen to be 10^{-4}.

We use these upper and lower bounds of the variables as the input arguments for gamultiobj to get the optimized values of variables of interest. Note that as we are performing multi-objective optimization, we get number of optimized solutions instead of a unique solution. The objective function values corresponding to these optimal solutions are shown in Fig. 9 in the form of Pareto front for three different frequency ranges. From Fig. 9, we can observe that there is always a tradeoff between two objective functions, i.e., a true minima point of T_{pw} does not coincide with true minima of T_{fw}. To elaborate this observation further, we show three different sets of optimal solutions for low, middle, and higher frequency ranges in Tables 2–4, respectively. We emphasize that although all three sets are feasible solution to our optimization problem, set 1 and set 3 correspond to min T_{pw} and min T_{fw}, respectively, while set 2 provides tradeoff values of T_{fw} and T_{pw}. To avoid any preference of one objective element over another element, we have used set 2 as our optimized solution candidate for further analysis.

Furthermore, from Tables 2 and 4, we can observe that optimum values of k_6 and k_7 settle down to their high and lower bounds for low and high-frequency ranges, respectively. This observation can be justified from the aspect of vibration isolation of single degree-of-freedom system. In an isolation zone (higher frequency range in our case), lower stiffness of isolator leads to better isolation; however, for very low excitation frequencies, high stiffness of the isolator provides better performance. Having established the solution candidate for the optimized glove, next

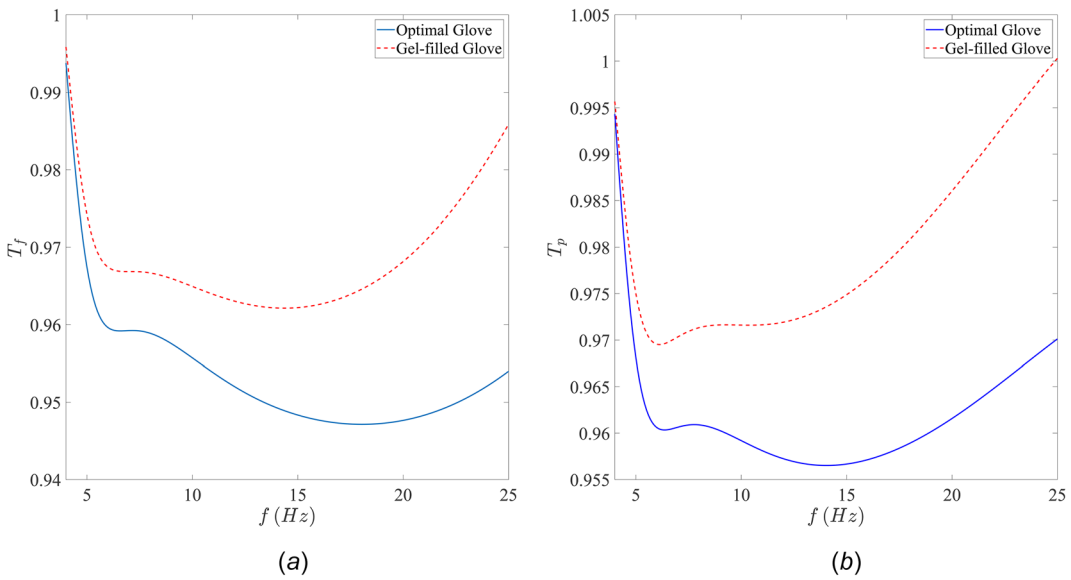

Fig. 10 Comparison of relative (*a*) finger transmissibility and (*b*) palm transmissibility curves for the optimum glove parameters and glove parameters used in Table 1. Optimization of the glove parameters is performed for low-frequency range.

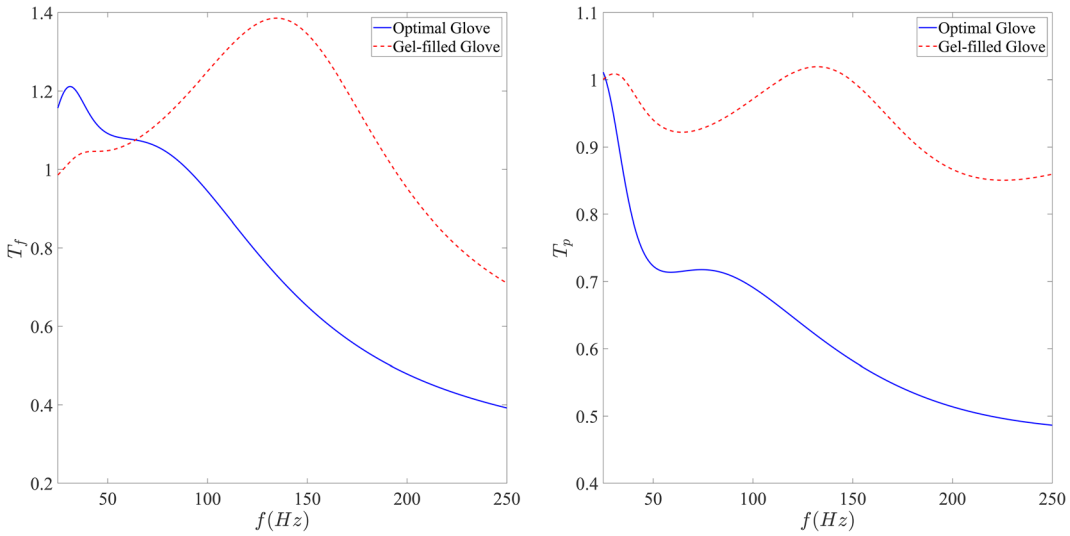

Fig. 11 Comparison of relative (*a*) finger transmissibility and (*b*) palm transmissibility curves for the optimum glove parameters and glove parameters used in Table 1. Optimization of the glove parameters is performed for medium-frequency range.

we present the comparison of the performance of optimized glove against the gel-filled glove. For this, we compare the relative transmissiblity for the optimized glove and gel-filled glove in low, medium, and high-frequency ranges and are shown in Figs. 10–12, respectively.

From Fig. 10, we can observe that the antivibration glove, with optimum glove parameters, is more effective at attenuating vibrations in the low-frequency region at the fingers than the antivibration glove described in Table 1. The optimized antivibration glove isolates rather than amplify vibration to the finger unlike most typical antivibration gloves [33].

In both the medium and high-frequency ranges as seen in Fig. 11, the optimal AV glove performs better than the glove described in Table 1. Therefore, an antivibration glove designed with these parameters may help attenuate high-frequency vibrations from tools such as etching pens, rotary files, and chainsaws.

Even though the optimized AV glove parameters presented above may not be physically realizable, the multi-objective study reveals what parameters of a real-life AV glove could be changed so as to improve its performance. For example, considering the low-frequency range optimal parameter values on the pareto front for k_4 (set 1 and set 2), it can be observed that reducing the stiffness of the glove material at the backside of the hand, k_4, will result in a glove that provides better palm transmissibility, but worse finger transmissibility. As a result, a manufacturer may decide to replace the back of a current glove material with a material of lower stiffness so as to increase the effectiveness of the glove in reducing vibrations to the palm. Through observing how

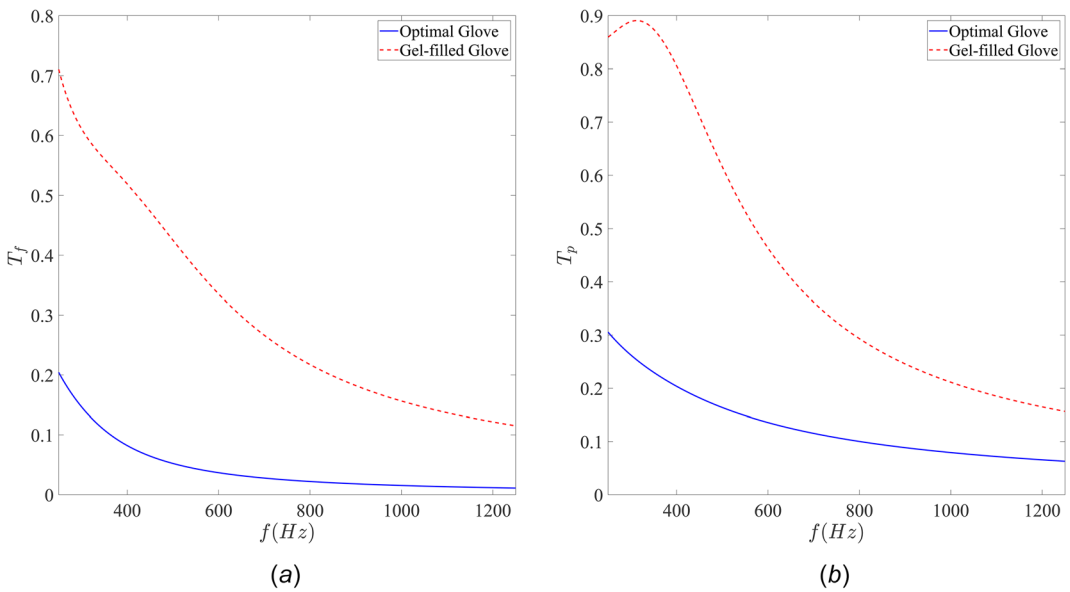

Fig. 12 Comparison of relative (*a*) finger transmissibility and (*b*) palm transmissibility curves for the optimum glove parameters and glove parameters used in Table 1. Optimization of the glove parameters is performed for high-frequency range.

glove material properties differ for different pareto sets, glove manufacturers can select glove materials which enhance or degrade transmissibility at either the palm or finger, depending on their needs.

It should be noted that the optimized AV gloves for the different frequency ranges might be effective, provided they are able to meet ergonomic constraints (e.g., manual dexterity, percent reduction in grip strength, and tool controllability) so as to ensure little to no possibility of injuries as a result of using the gloves.

Conclusion

We studied the vibration of the hand–arm system, using a biomechanical lumped parameter model of the system, with and without gloves. For the current analysis, the interaction between different parts of the human hand and hand–tool was considered to be linear for simplicity. These linear interactions were modeled as multiple linear springs and dampers, making the system a multidegree-of-freedom system. The closed-form solution for the responses of the hand–arm system was obtained using the method of undetermined coefficients. The obtained analytical expressions were validated using direct numerical simulations, and the results showed very good agreement. The effect of different glove parameters on the transmissibility of the palm was investigated with and without a glove. The results further suggested that the effect of the glove was not monotonous for the given frequency range. Therefore, it was necessary to analyze the glove parameter based on the application and frequency. With this motivation, we optimized the glove parameter for three different frequency ranges with predefined upper and lower bounds to minimize the overall transmissibility. We observed that for these optimum values the transmissibility at higher frequencies was minimum as compared to the values used in the earlier work. The implication here is that the AV glove with this optimum values can be used to design gloves to protect workers from high-frequency vibrations from tools such as etching pens, rotary files, and chainsaws.

Appendix: Expressions Used in Eqs. (5) and (10)

$$[\mathbf{M}] = \begin{bmatrix} m_0 & 0 & 0 & 0 \\ 0 & m_f & 0 & 0 \\ 0 & 0 & m_p & 0 \\ 0 & 0 & 0 & m_{\text{tf}} + m_{\text{tp}} + m_H \end{bmatrix}$$

$$[\mathbf{C}] = \begin{bmatrix} c_0 + c_w & 0 & -c_w & 0 \\ 0 & c_1 + c_2 & -c_1 & -c_2 \\ -c_w & -c_1 & c_w + c_1 + c_3 & -c_3 \\ 0 & -c_2 & -c_3 & c_2 + c_3 + c_s \end{bmatrix}$$

$$[\mathbf{K}] = \begin{bmatrix} k_0 + k_w & 0 & -k_w & 0 \\ 0 & k_1 + k_2 & -k_1 & -k_2 \\ -k_w & -k_1 & k_w + k_1 + k_3 & -k_3 \\ 0 & -k_2 & -k_3 & k_2 + k_3 + k_s \end{bmatrix}$$

$$[\mathbf{F}_{\text{eq}}] = \begin{bmatrix} 0 \\ 0 \\ 0 \\ c_s\dot{z} + k_s z \end{bmatrix}$$

$$[\mathbf{M}_1] = \begin{bmatrix} m_0 & 0 & 0 & 0 & 0 & 0 \\ 0 & m_f + m_{g1} & 0 & 0 & 0 & 0 \\ 0 & 0 & m_p + m_{g2} & 0 & 0 & 0 \\ 0 & 0 & 0 & m_{\text{tp}} + m_{g4} & 0 & 0 \\ 0 & 0 & 0 & 0 & m_{\text{tf}} + m_{g3} & 0 \\ 0 & 0 & 0 & 0 & 0 & m_{g5} + m_{g6} + m_H \end{bmatrix}$$

$$[\mathbf{C}_1] = \begin{bmatrix} \mathbf{C1} & \mathbf{C2} \\ \mathbf{C2}^{\text{T}} & \mathbf{C3} \end{bmatrix}$$

$$[\mathbf{C1}] = \begin{bmatrix} c_0 + c_w & 0 & -c_w \\ 0 & c_1 + c_4 + c_2 & -c_1 - c_4 \\ -c_w & -c_1 - c_4 & c_1 + c_4 + c_3 + c_w \end{bmatrix}$$

$$[\mathbf{C2}] = \begin{bmatrix} 0 & 0 & 0 \\ 0 & -c_2 & 0 \\ -c_3 & 0 & 0 \end{bmatrix}$$

$$[\mathbf{C3}] = \begin{bmatrix} c_3 + c_5 + c_7 & -c_5 & -c_7 \\ -c_5 & c_2 + c_5 + c_6 & -c_6 \\ -c_7 & -c_6 & c_6 + c_7 + c_s \end{bmatrix}$$

$$[\mathbf{K}_1] = \begin{bmatrix} \mathbf{K1} & \mathbf{K2} \\ \mathbf{K2}^{\text{T}} & \mathbf{K3} \end{bmatrix}$$

$$[\mathbf{K1}] = \begin{bmatrix} k_0 + k_w & 0 & -k_w \\ 0 & k_1 + k_4 + k_2 & -k_1 - k_4 \\ -k_w & -k_1 - k_4 & k_1 + k_4 + k_3 + k_w \end{bmatrix}$$

$$[\mathbf{K2}] = \begin{bmatrix} 0 & 0 & 0 \\ 0 & -k_2 & 0 \\ -k_3 & 0 & 0 \end{bmatrix}$$

$$[\mathbf{K3}] = \begin{bmatrix} k_3 + k_5 + k_7 & -k_5 & -k_7 \\ -k_5 & k_2 + k_5 + k_6 & -k_6 \\ -k_7 & -k_6 & k_6 + k_7 + k_s \end{bmatrix}$$

References

[1] Su, A. T., Maeda, S., Fukumoto, J., Darus, A., Hoe, V. C. W., Miyai, N., Isahak, M., Takemura, S., Bulgiba, A., Yoshimasu, K., and Miyashita, K., 2013, "Dose–Response Relationship Between Hand-Transmitted Vibration and Hand-Arm Vibration Syndrome in a Tropical Environment," Occup. Environ. Med., **70**(7), pp. 498–504.

[2] Goglia, V., Gospodarić, Z., Košutić, S., and Filipović, D., 2003, "Hand-Transmitted Vibration From the Steering Wheel to Drivers of a Small Four-Wheel Drive Tractor," Appl. Ergon., **34**(1), pp. 45–49.

[3] Bovenzi, M., 2005, "Health Effects ofMechanical Vibration," G. Ital. Med. Lav. Ergon., **27**(1), pp. 58–64.

[4] Azmir, N., Ghazali, M., Yahya, M., Ali, M., and Song, J., 2015, "Effect of Hand Arm Vibration on the Development of Vibration Induce Disorder Among Grass Cutter Workers," Procedia Manuf., **2**, pp. 87–91.

[5] Mandal, B. B., and Srivastava, A. K., 2006, "Risk From Vibration in Indian Mines," Indian J. Occup. Environ. Med., **10**(2), pp. 53–57.

[6] Wikström, B.-O., Kjellberg, A., and Landström, U., 1994, "Health Effects of Long-Term Occupational Exposure to Whole-Body Vibration: A Review," Int. J. Ind. Ergon., **14**(4), pp. 273–292.

[7] Kim, J. H., Aulck, L., Hughes, M., Zigman, M., Cavallari, J., Dennerlein, J. T., and Johnson, P. W., 2015, "Whole Body Vibration Exposures in Long-Haul Truck Drivers," Proceedings of the Human Factors and Ergonomics Society Annual Meeting, Vol. 59, SAGE Publications Sage CA, Los Angeles, CA, Oct. 26–30, pp. 1274–1278.

[8] Marin, L. S., Rodriguez, A. C., Rey-Becerra, E., Piedrahita, H., Barrero, L. H., Dennerlein, J. T., and Johnson, P. W., 2017, "Assessment of Whole-Body Vibration Exposure in Mining Earth-Moving Equipment and Other Vehicles Used in Surface Mining," Ann. Work Exposures Health, **61**(6), pp. 669–680.

[9] Zaka, M. Z., Saleem, M. S., Khaliq, A., and Afzal, M., 2014, "Effect of Hand Transmitted Vibration Through Tractor During Ploughing Field," Int. J. Eng. Res. Appl., **4**(12), pp. 18–23.

[10] Hulshof, C., 1986, "Whole-Body Vibration and Low Back Pain: A Review of Epidemilogic Studies," Int. Arch. Occup. Environ. Health, **58**, pp. 1–12.
[11] Kim, J. H., Marin, L. S., and Dennerlein, J. T., 2018, "Evaluation of Commercially Available Seat Suspensions to Reduce Whole Body Vibration Exposures in Mining Heavy Equipment Vehicle Operators," Appl. Ergon., **71**, pp. 78–86.
[12] Griffin, M., Bovenzi, M., and Nelson, C., 2003, "Dose-Response Patterns for Vibration-Induced White Finger," Occup. Environ. Med., **60**(1), pp. 16–26.
[13] Dong, R. G., Wu, J. Z., and Welcome, D. E., 2005, "Recent Advances in Biodynamics of Human Hand-Arm System," Ind. Health, **43**(3), pp. 449–471.
[14] Barregard, L., Ehrenström, L., and Marcus, K., 2003, "Hand-Arm Vibration Syndrome in Swedish Car Mechanics," Occup. Environ. Med., **60**(4), pp. 287–294.
[15] Vihlborg, P., Bryngelsson, L., Lindgren, B., Gunnarsson, L. G., and Graff, P., 2017, "Association Between Vibration Exposure and Hand-Arm Vibration Symptoms in a Swedish Mechanical Industry," Int. J. Ind. Ergon., **62**, pp. 77–81.
[16] Gemne, G., Saraste, H., Christ, E., and Dupuis, H. G., 1987, "Bone and Joint Pathology in Workers Using Hand-Held Vibrating Tools: An Overview [With Discussion]," Scand. J. Work, Environ. Health, **13**(4), pp. 290–300.
[17] Hao, K. Y., Mei, L. X., and Ripin, Z. M., 2011, "Tuned Vibration Absorber for Suppression of Hand-Arm Vibration in Electric Grass Trimmer," Int. J. Ind. Ergon., **41**(5), pp. 494–508.
[18] Zardin, B., Borghi, M., Gherardini, F., and Zanasi, N., 2018, "Modelling and Simulation of a Hydrostatic Steering System for Agricultural Tractors," Energies, **11**(1), p. 230.
[19] Dewangan, K., and Tewari, V., 2009, "Characteristics of Hand-Transmitted Vibration of a Hand Tractor Used in Three Operational Modes," Int. J. Ind. Ergon., **39**(1), pp. 239–245.
[20] Dong, R., Rakheja, S., McDowell, T., Welcome, D., Wu, J., Warren, C., Barkley, J., Washington, B., and Schopper, A., 2005, "A Method for Assessing the Effectiveness of Anti-Vibration Gloves Using Biodynamic Responses of the Hand–Arm System," J. Sound Vib., **282**(3–5), pp. 1101–1118.
[21] Hewitt, S., Dong, R., McDowell, T., and Welcome, D., 2016, "The Efficacy of Anti-Vibration Gloves," Acoust. Aust., **44**(1), pp. 121–127.
[22] Yao, Y., Rakheja, S., Gauvin, C., Marcotte, P., and Hamouda, K., 2018, "Evaluation of Effects of Anti-Vibration Gloves on Manual Dexterity," Ergonomics, **61**(11), pp. 1530–1544.
[23] Rezali, M., Anas, K., and Griffin, M. J., 2014, "The Transmission of Vibration Through Gloves to the Hand and to the Fingers: Effects of Material Dynamic Stiffness," Appl. Mech. Mater., **564**, pp. 149–154.
[24] Md Rezali, K. A., and Griffin, M. J., 2016, "Transmission of Vibration Through Gloves: Effects of Material Thickness," Ergonomics, **59**(8), pp. 1026–1037.
[25] Md Rezali, K. A., and Griffin, M. J., 2018, "Transmission of Vibration Through Glove Materials: Effects of Contact Force," Ergonomics, **61**(9), pp. 1246–1258.
[26] Welcome, D. E., Dong, R. G., Xu, X. S., Warren, C., and McDowell, T. W., 2014, "The Effects of Vibration-Reducing Gloves on Finger Vibration," Int. J. Ind. Ergon., **44**(1), pp. 45–59.
[27] Hamouda, K., Rakheja, S., Dewangan, K., and Marcotte, P., 2018, "Fingers' Vibration Transmission and Grip Strength Preservation Performance of Vibration Reducing Gloves," Appl. Ergon., **66**, pp. 121–138.
[28] Dong, J. H., Dong, R. G., Rakheja, S., Welcome, D. E., McDowell, T. W., and Wu, J. Z., 2008, "A Method for Analyzing Absorbed Power Distribution in the Hand and Arm Substructures When Operating Vibrating Tools," J. Sound Vib., **311**(3–5), pp. 1286–1304.
[29] Dong, R. G., McDowell, T. W., Welcome, D. E., Warren, C., Wu, J. Z., and Rakheja, S., 2009, "Analysis of Anti-Vibration Gloves Mechanism and Evaluation Methods," J. Sound Vib., **321**(1–2), pp. 435–453.
[30] Adewusi, S., Rakheja, S., Marcotte, P., and Boutin, J., 2010, "Vibration Transmissibility Characteristics of the Human Hand–Arm System Under Different Postures, Hand Forces and Excitation Levels," J. Sound Vib., **329**(14), pp. 2953–2971.
[31] Adewusi, S., Rakheja, S., and Marcotte, P., 2012, "Biomechanical Models of the Human Hand-Arm to Simulate Distributed Biodynamic Responses for Different Postures," Int. J. Ind. Ergon., **42**(2), pp. 249–260.
[32] Pinto, I., Stacchini, N., Bovenzi, M., Paddan, G., and Griffin, M., 2001, "Protection Effectiveness of Anti-Vibration Gloves: Field Evaluation and Laboratory Performance Assessment," Proceedings of the Ninth International Conference on Hand-Arm Vibration, Nancy, France, June 5–8, pp. 387–396.
[33] Dong, R., McDowell, T., Welcome, D., Smutz, W., Schopper, A., Warren, C., Wu, J., and Rakheja, S., 2003, "On-the-Hand Measurement Methods for Assessing Effectiveness of Anti-Vibration Gloves," Int. J. Ind. Ergon., **32**(4), pp. 283–298.
[34] McDowell, T. W., Dong, R. G., Welcome, D. E., Xu, X. S., and Warren, C., 2013, "Vibration-Reducing Gloves: Transmissibility at the Palm of the Hand in Three Orthogonal Directions," Ergonomics, **56**(12), pp. 1823–1840.
[35] Gupta, S. K., Alabi, O., Kakou, P.-C., and Barry, O., 2019, "On the Modeling and Optimization of Anti-Vibration Gloves for Hand-Arm Vibration Control," ASME Paper No. DSCC2019-9094.
[36] Freund, M. K., Farzaneh Joubaneh, E. H., Barry, O. R., and Tanbour, E. Y., 2017, "Study of Vibration of Electric Power Steering Systems Using a Continuous System Model," ASME Paper No. IMECE2017-70755.
[37] Sakthivel, A., Sriraman, S., and Verma, R. B., 2012, "Study of Vibration From Steering Wheel of an Agricultural Tractor," SAE Int. J. Commer. Veh., **5**(2), pp. 441–454.
[38] Inman, D. J., and Singh, R. C., 1994, *Engineering Vibration*, Vol. 3, Prentice Hall, Englewood Cliffs, NJ.
[39] ISO, E., 2000, "Mechanical Vibration and Shock—Hand-Arm Vibration—Method for the Measurement and Evaluation of the Vibration Transmissibility of Gloves at the Palm of the Hand," European Committee for Standardization, Brussels, Belgium, Standard No. 10819 (1996).
[40] ISO, I., 2001, "Mechanical Vibration—Measurement and Evaluation of Human Exposure to Hand-Transmitted Vibration—Part 1: General Requirements," International Organization for Standardization, Geneva, Switzerland, Standard No. 5349–1.
[41] Wimer, B., McDowell, T. W., Xu, X. S., Welcome, D. E., Warren, C., and Dong, R. G., 2010, "Effects of Gloves on the Total Grip Strength Applied to Cylindrical Handles," Int. J. Ind. Ergon., **40**(5), pp. 574–583.